

NUMERICAL ANALYSIS OF THE CHARACTERISTICS OF GLASS PHOTONIC CRYSTAL FIBERS INFILTRATED WITH ALCOHOLIC LIQUIDS

NGUYEN THI THUY¹, CHU THI GIA TRANG², LE VAN MINH², TRAN QUOC VU³,
NGUYEN THE MANH⁴, DOAN QUOC KHOA⁵, DINH XUAN KHOA⁶,
CHU VAN LANH^{6,†} AND LE TRAN BAO TRAN¹

¹*Hue University of Education, Hue University, 34 Le Loi, Hue City, Vietnam C*

²*School of Engineering and Technology, Vinh University, 182 Le Duan, Vinh city, Vietnam*

³*Thu Khoa Nghia High School for The Gifted, Chau Doc City, Vietnam*

⁴*Hong Duc University, 565 Quang Trung, Thanh Hoa, Vietnam*

⁵*Quang Tri Teacher Training College, Dong Ha, Quang Tri, Vietnam*

⁶*Department of Physics, Vinh University, 182 Le Duan, Vinh City, Vietnam*

[†]*E-mail: chuvanlanh@vinhuni.edu.vn*

Received 8 February 2020

Accepted for publication 17 March 2020

Published 25 July 2020

Abstract. *The characteristics of photonic crystal fibers (PCFs) with various air hole diameters infiltrated with alcoholic liquids such as ethanol, methanol, propanol and butanol are numerically investigated. Based on the numerical results, we have analyzed and compared in detail the characteristics of these fibers including effective refractive index, effective mode area, dispersion and confinement loss for two sets of parameters $\{d, \Lambda\} = \{1 \mu\text{m}, 5 \mu\text{m}\}$ and $\{1.42 \mu\text{m}, 3.26 \mu\text{m}\}$, with d the air hole diameter and Λ the lattice constant, respectively. The PCF infiltrated with ethanol and butanol shows better near zero flattened dispersion property at $1.42 \mu\text{m}$ and $1 \mu\text{m}$ wavelength, respectively. The values of effective refractive index, effective mode area, dispersion and confinement loss decrease in an orderly manner from butanol, propanol, ethanol to methanol and all the alcoholic liquid's curves of dispersion are flat and are very close to each other and near the zero dispersion curve. The proposed PCF shows a promising prospect in technology applications such as supercontinuum generation.*

Keywords: Photonic crystal fiber, effective refractive index, effective mode area, dispersion, confinement loss, nonlinear optics.

Classification numbers: 42.81.-i, 42.81.Wg..

I. INTRODUCTION

The idea of the first PCF was proposed by Yeh and his partners [1] in 1978, the core of the fiber was wrapped with a Bragg grating, similar to a one-dimensional photonic crystal. Photonic crystal fibers were made of photonic crystals with an air-core invented by Russell in 1992 and the first PCF with hexagonal structure was reported in the conference about optical fiber (OFC) in 1996 by Russell and colleagues [2], a new type of fiber. By cleverly disposing the structure, it is possible to design the fibers to have desired transmission properties. PCFs that are designed and manufactured may not disperse, lowly disperse, or extraordinarily (irregularly) disperse at the visible wavelength range. Dispersion can also be spread over a very wide range. The combination of irregular dispersion with small mode field areas is noted in non-linear fibers. Due to the structural diversity and geometrical parameters behaviors of PCF are qualified. The PCF studying focused on air-injected fibers and achieved encouraging results [3–5]. However, when using gas, there are some limitations such as: the dispersion lines with high slope, narrow dispersion wavelength range, nonlinearity in small PCF gas, so they have limitations when applied for super continuous emission. In recent years, many studies about PCF infiltrated with different liquids have been of particular interest because it not only overcomes the limitations of gas PCF but also opens up promising new applications in both fundamental research and device applications [6, 7]. The PCFs have been extended the range of possibilities in optical fibers by improving well-established properties such as geometry [8], confinement loss [9], possibility of broadband infrared supercontinuum generation [10], dispersion engineering [11], temperature sensitivity [12], influence of temperature [13], optimization of optical properties [14]. Applications of PCF include lasers, amplifiers, dispersion compensators, and nonlinear processing, optical devices [15], electrically tunable [16, 17], ultra-flattened-dispersion [18, 19], optofluidic device [20], dispersion compensation [21], and supercontinuum generation devices [22, 23].

The property of a PCF is determined by the diameter of holes and lattices constant. The effective cladding index of PCF can be flexibly controlled by adjusting the hole diameter (d) and lattice constant (Λ) of their air hole arrays in the cladding [4, 24]. Due to a relatively high non-linear refractive index of alcohols solution in comparison with solids (it is even up to 100 times larger than that in fused silica [25]), alcohols solution would be the most basic liquids for many applications because they comprise the vast majority of biological or chemical solutions and generating supercontinuum [12–14]. In this study, we design and optimize an air-glass fiber structure infiltrated with alcoholic liquids such as ethanol, methanol, propanol, butanol. The characteristics for PCF infiltrated with alcoholic liquids with various air hole diameters and lattice constants were compared.

II. MODELING AND THEORY

Figure 1 shows the geometrical structure of the solid core-PCF. A PCF with regular hexagonal with air holes either empty or infiltrated with ethanol, methanol, propanol, butanol solutions. In previous studies [12, 13, 26], authors have optimized the optical properties of PCF infiltrated with water or ethanol with $\Lambda = 3.26 \mu\text{m}$, $5.0 \mu\text{m}$ and $d = 1.0 \mu\text{m}$, $1.42 \mu\text{m}$. Thus, the PCF structure was designed with 8 rings of air holes, the diameter of air holes and the lattice constants are chosen as $\{\Lambda, d\} = \{3.26 \mu\text{m}, 1.42 \mu\text{m}\}$ and $\{5.0 \mu\text{m}, 1.0 \mu\text{m}\}$ for alcoholic liquids.

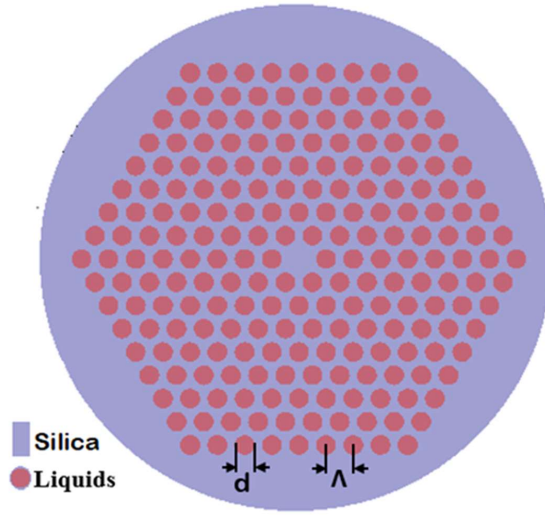


Fig. 1. The geometrical structures of solid core-PCFs with hexagonal lattices in the cladding infiltrated with alcoholic liquids.

The finite difference method to solve Maxwell’s equation on a cross-section of the PCF fiber waveguide was used to model. Mathematically, by solving the Maxwell equation, an eigenvalue equation is formed. Therefore, the differential equations are converted into a matrix eigenvalue equation. In addition, the mode profiles, which are associated with the eigenvectors, and the propagation constants, which correspond to the eigenvalues, are calculated. In this study, the characteristics of the PCF structure such as effective refractive index, effective mode area, dispersion, and confinement loss were calculated by using Lumerical Model Solution software [27].

The refractive index of a few guided modes is plotted in Fig. 2 as a function of wavelength. Sellmeier’s equations (1) and (2) [28] show the dependence of refractive index on wavelength for ethanol, methanol, propanol and butanol respectively.

The Sellmeier’s equation for ethanol:

$$n_{Ethanol}^2(\lambda) = 1 + \frac{A_{11}\lambda^2}{\lambda^2 - B_{11}} + \frac{A_{21}\lambda^2}{\lambda^2 - B_{21}}, \tag{1}$$

with coefficients: $A_{11} = 0.83189$, $B_{11} = 0.00930 \mu\text{m}^2$, $A_{21} = -0.15582$, $B_{21} = -49.4520 \mu\text{m}^2$

The Sellmeier’s equation for methanol, propanol and butanol:

$$n^2(\lambda) = A_0 + A_1\lambda^2 + \frac{A_2}{\lambda^2} + \frac{A_3}{\lambda^4} + \frac{A_4}{\lambda^6}, \tag{2}$$

where A_i are the coefficients, as illustrated in Table 1

With the fused silica, refractive index can be obtained using Cauchy’s equation (3) [29], where λ is the wavelength in micrometers.

$$n_{Fused\ silica}^2(\lambda) = B_0 + \frac{B_1\lambda^2}{\lambda^2 - C_1} + \frac{B_2\lambda^2}{\lambda^2 - C_2} + \frac{B_3\lambda^2}{\lambda^2 - C_3}, \tag{3}$$

with coefficients: $B_0 = 1$; $B_1 = 0.6694226$, $B_2 = 0.4345839$, $B_3 = 0.8716947$, $C_1 = 4.4801 \times 10^{-3} \mu\text{m}^2$, $C_2 = 1.3285 \times 10^{-2} \mu\text{m}^2$, $C_3 = 95.341482 \mu\text{m}^2$.

An important quantity in designing PCF is the effective mode area (A_{eff}). A_{eff} is characteristic nonlinearity of PCF. It is related to the effective area of the core area defined as following (4) [30]:

$$A_{eff} = \frac{\left(\int_{-\infty}^{\infty} \int_{-\infty}^{\infty} |E|^2 dx dy \right)^2}{\int_{-\infty}^{\infty} \int_{-\infty}^{\infty} |E|^4 dx dy}, \quad (4)$$

where E is the electric field amplitude.

To evaluate the broadening or spreading of light propagating inside the PCF, chromatic dispersion (D) can be used in investigating the dispersion properties of the PCF, the dispersion is calculated in [30], which is defined as

$$D = -\frac{\lambda}{c} \frac{d^2 \text{Re} [n_{eff}]}{d\lambda^2}, \quad (5)$$

where $\text{Re} [n_{eff}]$ is the real part of n_{eff} and c is the velocity of light in vacuum [20, 31].

Table 1. The value of Sellmeier coefficients for methanol, propanol and butanol

| Sellmeier coefficients | Methanol | Propanol | Butanol |
|------------------------|---------------------------------|---------------------------------|--------------------------------|
| A_0 | 1.745946239 | 1.893400242 | 1.917816501 |
| A_1 | $-0.005362181 \mu\text{m}^{-2}$ | $-0.003349425 \mu\text{m}^{-2}$ | $-0.00115077 \mu\text{m}^{-2}$ |
| A_2 | $0.004656355 \mu\text{m}^2$ | $0.004418653 \mu\text{m}^2$ | $0.01373734 \mu\text{m}^2$ |
| A_3 | $0.00044714 \mu\text{m}^4$ | $0.00108023 \mu\text{m}^4$ | $-0.00194084 \mu\text{m}^4$ |
| A_4 | $-0.000015087 \mu\text{m}^6$ | $-0.000067337 \mu\text{m}^6$ | $0.000254077 \mu\text{m}^6$ |

The other property of the PCF is confinement loss (L_c) created from the leakage of the modes and the structure of the PCF [32]. It can be calculated by the following equation

$$L_c = 8.686k_0 \text{Im} [n_{eff}] \text{ (dB/m)}, \quad (6)$$

where $\Im [n_{eff}]$ is the imaginary part of n_{eff} [33].

The real parts of refractive index of ethanol, methanol, propanol, butanol and fused silica [28, 29] are shown in Fig. 2. Reliable data are available only for the wavelength range of $0.4 \mu\text{m}$ - $1.8 \mu\text{m}$, so we limited the simulation to this range.

In addition, the characteristics of the PCF can be flexibly controlled by adjusting the hole diameter and lattices constant of air hole arrays in the cladding, especially these properties are usually strongly dependent on infiltrating liquids such as ethanol, methanol, propanol and butanol. These characteristics have been thoroughly investigated in this study.

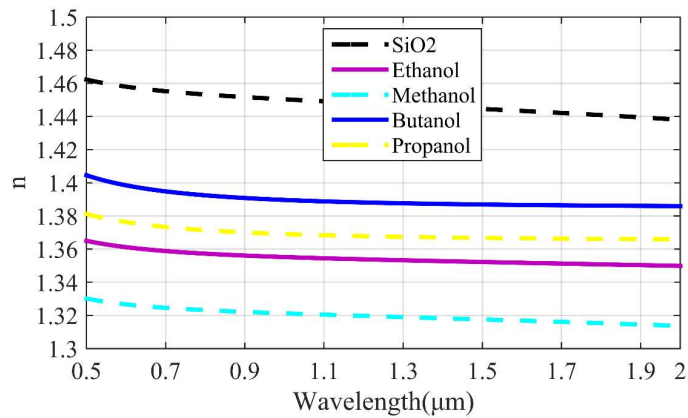


Fig. 2. Real parts of refractive index of alcoholic liquids and silica.

III. RESULTS AND DISCUSSION

III.1. Effective refraction index

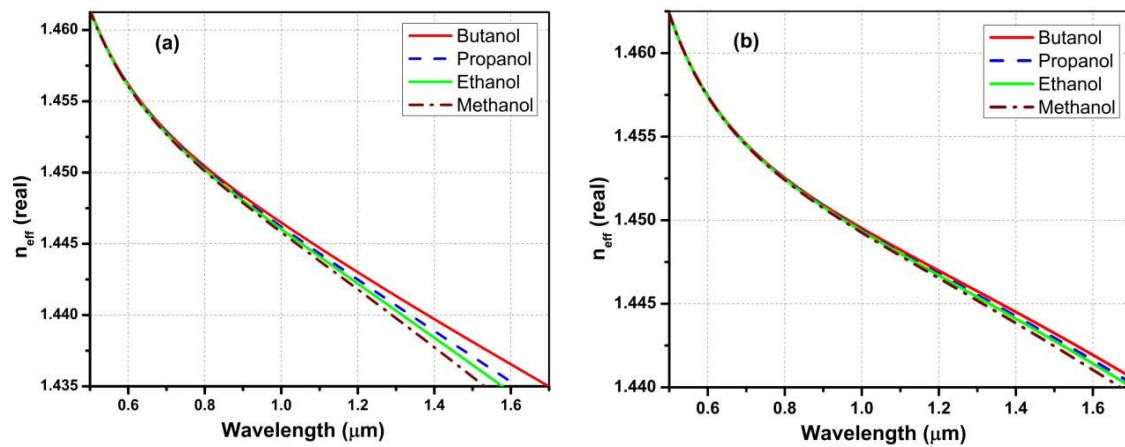


Fig. 3. Real part of effective refraction index as a function of wavelength of the fiber with various air hole diameters infiltrated with alcoholic liquids. a) $d = 1.42 \mu\text{m}$ and $\Lambda = 3.26 \mu\text{m}$ and b) $d = 1 \mu\text{m}$ and $\Lambda = 5 \mu\text{m}$

Figure 3 presents the effective refraction index (n_{eff}) of fundamental modes in the PCF infiltrated with ethanol, methanol, propanol, butanol in two cases: a) $d = 1.42 \mu\text{m}$, $\Lambda = 3.26 \mu\text{m}$ and b) $d = 1 \mu\text{m}$, $\Lambda = 5 \mu\text{m}$. As seen in Fig. 3, the effective refraction index is changed with varying the wavelength and the alcoholic liquids. The effective refraction index decreases with increasing the wavelength and its value decreases in order from butanol to propanol, ethanol and methanol. Moreover, the effective refractive index of the fiber infiltrated with butanol is greatest

at the same value of wavelength and diameter of air holes because butanol's real part of refractive index is the largest at each wavelength.

As shown in Fig. 3a and 3b, the curves of the effective refractive index of the PCF infiltrated with butanol propanol, ethanol and methanol are very similar in shape. However, the curves in Fig. 3a are separated more clearly at 1.55 μm wavelength than the curves in Fig. 3b. When the diameter of air holes and lattices constant are 1.42 μm and 3.26 μm respectively, the curves are sloped so the effective refraction index of alcoholic liquids decreases quickly with increasing the wavelength (Fig.3a).

Table 2. The value of the effective refractive index of the fiber with various air hole diameters at 1.55 μm wavelength infiltrated with alcoholic liquids.

| λ (μm) | Liquids | n_{eff} | |
|-----------------------------|----------|---|---|
| | | $d = 1.42 \mu\text{m}$ and $\Lambda = 3.26 \mu\text{m}$ | $d = 1 \mu\text{m}$ and $\Lambda = 5 \mu\text{m}$ |
| 1.55 | Butanol | 1.4379267 | 1.44308356 |
| | Propanol | 1.43687585 | 1.44279326 |
| | Ethanol | 1.43626663 | 1.44261515 |
| | Methanol | 1.43539118 | 1.44228774 |

The value of the effective refractive index of the fiber with various air hole diameters at 1.55 μm wavelength infiltrated with alcoholic liquids are shown in Table 2. When the diameter of air holes and lattice constant are 1 μm and 5 μm respectively, the value of the effective refractive index of different liquids is greater than the other. In this case, the change in the effective refractive index among alcoholic liquids is the minimum value equal to 0.0002 and maximum value equal to 0.0007. Besides, the change in the effective refractive index among alcoholic liquids is the minimum value equal to 0.001 and maximum value equal to 0.002 when the diameter of air holes and lattice constant are 1.42 μm and 3.26 μm respectively.

III.2. Effective mode area

The dependence of effective mode area on the wavelength of the PCF infiltrated with alcoholic liquids is calculated with various diameters and lattice constants of air holes and shown in Fig. 4, its value increases with increasing of the wavelength and increases with decreasing of the diameter of the air holes from 1.42 μm to 1 μm . As observed, the curves present a different shape for the two cases of diameters and lattices constant of air holes, the increase of effective mode area corresponding to wavelength in case (b) is faster than in case (a) (Fig. 4a and 4b). On the other hand, the effective mode area of PCF infiltrated with butanol has the highest value among PCF infiltrated with different alcoholic liquids at the same value of both wavelength and diameter of the air holes. The value of effective mode area of cladding is reduced in order from butanol to propanol, ethanol, methanol similar to the effective refractive index.

Table 3 shows the effective mode area value of PCF infiltrated with alcoholic liquids. At the 1.55 μm wavelength, with the diameter of air holes of 1.0 μm and 1.42 μm , the highest effective mode area of butanol is 1202.32333 μm^2 and 71.041579 μm^2 , respectively, its value is reduced

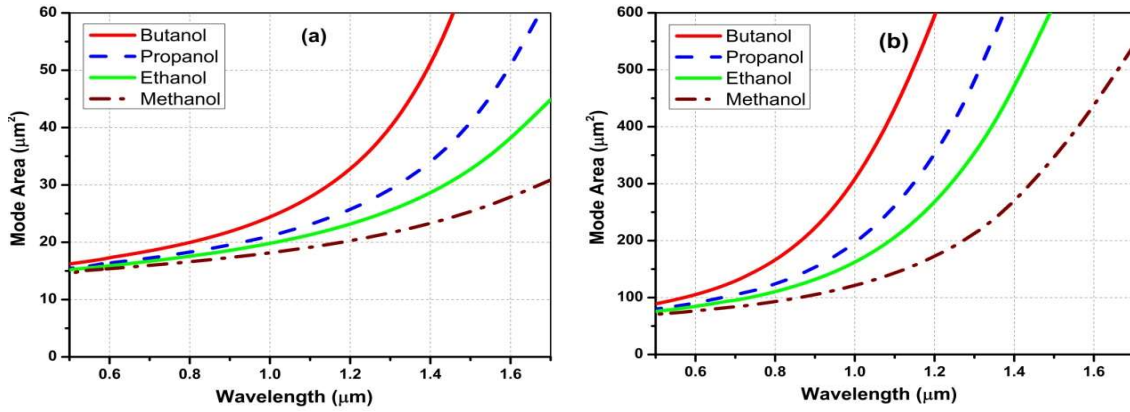


Fig. 4. Effective mode area as a function of wavelength of the fiber with various air hole diameters infiltrated with alcoholic liquids. a) $d = 1.42 \mu\text{m}$ and $\Lambda = 3.26 \mu\text{m}$ and b) $d = 1 \mu\text{m}$ and $\Lambda = 5 \mu\text{m}$.

about 17 times. Meanwhile, the lowest effective mode area of methanol is $357.116216 \mu\text{m}^2$ and $25.6336195 \mu\text{m}^2$, its value is reduced about 14 times. Similarly, the reduction of the effective mode area value for propanol is about 20 times, for ethanol is about 19 times. This is because, with the increase of diameters, the refractive index of alcoholic liquids decreases, the local capacity to light becomes strong, leading to reduction of the effective area, and the light field is more concentrated to the core and gradually away from the cladding layer, so the influence of liquid refractive index of the outer air hole on it is smaller and smaller [34].

Table 3. The value of the effective mode area of the fiber with various air hole diameters at $1.55 \mu\text{m}$ wavelength infiltrated with alcoholic liquids.

| $\lambda (\mu\text{m})$ | Liquids | $A_{eff}(\mu\text{m}^2)$ | |
|-------------------------|----------|---|---|
| | | $d = 1.42 \mu\text{m}$ and $\Lambda = 3.26 \mu\text{m}$ | $d = 1 \mu\text{m}$ and $\Lambda = 5 \mu\text{m}$ |
| 1.55 | Butanol | 71.041579 | 1202.32333 |
| | Propanol | 42.0205109 | 845.546951 |
| | Ethanol | 33.3779094 | 633.833495 |
| | Methanol | 25.6336195 | 357.116216 |

Therefore, we emphasize that it is possible to tailor the range of the effective mode area to be suitable to the needs of a specific application via varying the size of air hole diameters and the kind of liquid. The PCF with a large effective mode area is used for high-power applications such as laser welding and machining, optical lasers, and amplifiers due to these and nonlinear and fiber damage limitations [35,36]. Meanwhile, the PCF with small effective area fibers have a high density of power, thus are suitable for supercontinuum generation [37, 38].

III.3. Chromatic dispersion

Figure 5 depicts the chromatic dispersion of the PCF as a function of wavelength. The dispersion slope is large in the wavelength range from $0.5 \mu\text{m}$ to $0.9 \mu\text{m}$ and it becomes smooth and close to zero in the wavelength range from $0.9 \mu\text{m}$ to $1.6 \mu\text{m}$. The results show that the shape of the dispersion characteristics for both diameters and lattice constants of air holes is different. When the diameters and lattice constants of air holes are equal to $1.42 \mu\text{m}$ and $3.26 \mu\text{m}$ (Fig. 5a), curves of the chromatic dispersion are clearly separated in the wavelength range from $0.9 \mu\text{m}$ to $1.6 \mu\text{m}$, butanol and propanol's curves do not cross the zero dispersion wavelength meanwhile curves of ethanol and methanol are flat and very close to the zero dispersion wavelength. With the wavelength higher than $1.2 \mu\text{m}$, the value of the dispersion of methanol is highest for all cases, the flattest dispersion curve, the nearest with the zero dispersion curve and the smallest of the dispersion's value is for ethanol in case (a) (Fig. 5a), it is due to the fact that the molecular density of methanol is higher than that of the others, in consistence with the publication [26].

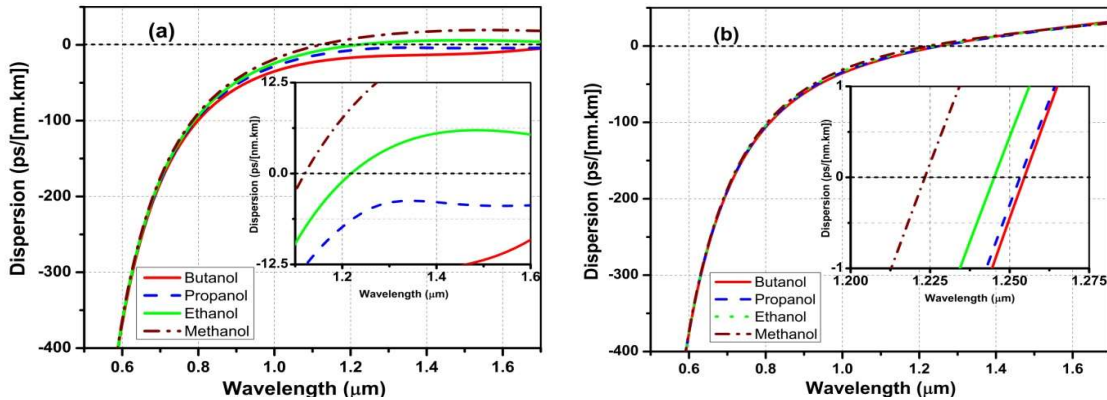


Fig. 5. Chromatic dispersion as a function of wavelength of the fiber with various air hole diameters infiltrated with alcoholic liquids. a) $d = 1.42 \mu\text{m}$ and $\Lambda = 3.26 \mu\text{m}$ and b) $d = 1 \mu\text{m}$ and $\Lambda = 5 \mu\text{m}$.

In contrast, when the diameters and lattice constants of air holes are respectively equal to $1 \mu\text{m}$ and $5 \mu\text{m}$ (Fig.5b), the chromatic dispersion curves of alcoholic liquids are quite close to each other, these curves are flat close to the zero dispersion wavelength in the range from $0.9 \mu\text{m}$ to $1.6 \mu\text{m}$. Furthermore, at the same value of wavelength and diameter of the air holes, values of dispersion of PCF infiltrated with alcoholic liquids are approximately equal, indicating that the PCF filled with butanol exhibits better near zero flattened dispersion characteristics. The PCF with the diameter of $1.0 \mu\text{m}$ and lattice constant of $5 \mu\text{m}$ of air holes for all liquids exhibits the flattest dispersed curve and the nearest with the zero dispersion curve; in this case, the dispersion curves are optimal, which is very useful for optical information and supercontinuum generation at near-infrared range.

In Table 4, the calculated values of dispersion for both cases at $1.55 \mu\text{m}$ wavelength are shown. As seen in Table 4, with diameter and lattice constant of air holes of $1.42 \mu\text{m}$ and $3.26 \mu\text{m}$, the smallest dispersion of PCF filled with ethanol of $5.91075308 \text{ (ps.(nm.km)}^{-1})$ and methanol of $19.3592474 \text{ (ps.(nm.km)}^{-1})$ can be obtained. The value of butanol and propanol's

dispersion is negative and changing the sign of the dispersion as the diameter is decreasing to 1 μm . With decreasing the diameter of air holes to 1 μm , the PCF filled with alcoholic liquids shows that the dispersion values are approximately equal (from 20.4739599 to 19.2975427 ($\text{ps} \cdot (\text{nm} \cdot \text{km})^{-1}$)). Comparing the value of dispersion of methanol and ethanol between two cases for the diameter of air holes, the difference in value of the dispersion is not great for the methanol (equal 0.9959 ($\text{ps} \cdot (\text{nm} \cdot \text{km})^{-1}$)), however, the difference for ethanol is quite large (equal 13.9324 ($\text{ps} \cdot (\text{nm} \cdot \text{km})^{-1}$)).

Table 4. The value of the chromatic dispersion of the fiber with various air hole diameters at 1.55 μm wavelength infiltrated with alcoholic liquids.

| λ (μm) | Liquids | D ($\text{ps} \cdot (\text{nm} \cdot \text{km})^{-1}$) | |
|-----------------------------|----------|--|---|
| | | d = 1.42 μm and $\Lambda = 3.26 \mu\text{m}$ | d = 1 μm and $\Lambda = 5 \mu\text{m}$ |
| 1.55 | Butanol | -11.6359866 | 20.4739599 |
| | Propanol | -4.42499772 | 19.2975427 |
| | Ethanol | 5.91075308 | 19.8431732 |
| | Methanol | 19.3592474 | 20.3551617 |

The proposed PCF which is filled with alcoholic liquids exhibits the zero dispersion (ZDW) in the near-infrared range as shown in Table 5. The ZDW of the PCF infiltrated with ethanol is higher than that of the PCF infiltrated with methanol for two cases of various air hole diameters. Moreover, with increasing diameter of air-holes, the ZDW of PCF decreases for both methanol and ethanol, the same phenomenon was observed in the PCF filled with water [13], the highest ZDW of the PCF infiltrated with ethanol and methanol is 1.24604224 μm and 1.22405714 μm , respectively. With the diameter of air holes of 1.42 μm , the value of the ZDW of butanol and propanol cannot be determined but these values are 1.254266549 μm and 1.25374947 μm for butanol and propanol at the 1 μm diameter of air holes, respectively. Moreover, the reduction of the ZDW's values of the fiber with various air hole diameters infiltrated with alcoholic liquids is in order from butanol, propanol, ethanol to methanol.

Table 5. The value of the zero dispersion wavelength (ZDW) of the fiber with various air hole diameters infiltrated with alcoholic liquids.

| Liquids | ZDW (μm) | |
|----------|---|---|
| | d = 1.42 μm and $\Lambda = 3.26 \mu\text{m}$ | d = 1 μm and $\Lambda = 5 \mu\text{m}$ |
| Butanol | - | 1.25426654 |
| Propanol | - | 1.25374947 |
| Ethanol | 1.21868795 | 1.24604224 |
| Methanol | 1.12038063 | 1.22405714 |

III.4. Confinement loss

The confinement loss as a function of wavelength of the PCF with various air hole diameters is presented in Fig. 6, its value increases with increasing the wavelength and increases with decreasing the diameter of the air holes from $1.42 \mu\text{m}$ to $1 \mu\text{m}$. When the diameter and lattice constant of air holes are equal $1 \mu\text{m}$ and $5 \mu\text{m}$, the confinement loss curves are separated clearly. Especially, the confinement loss curves of butanol increase linearly with wavelength and its value is highest among the infiltrated with alcoholic liquids.

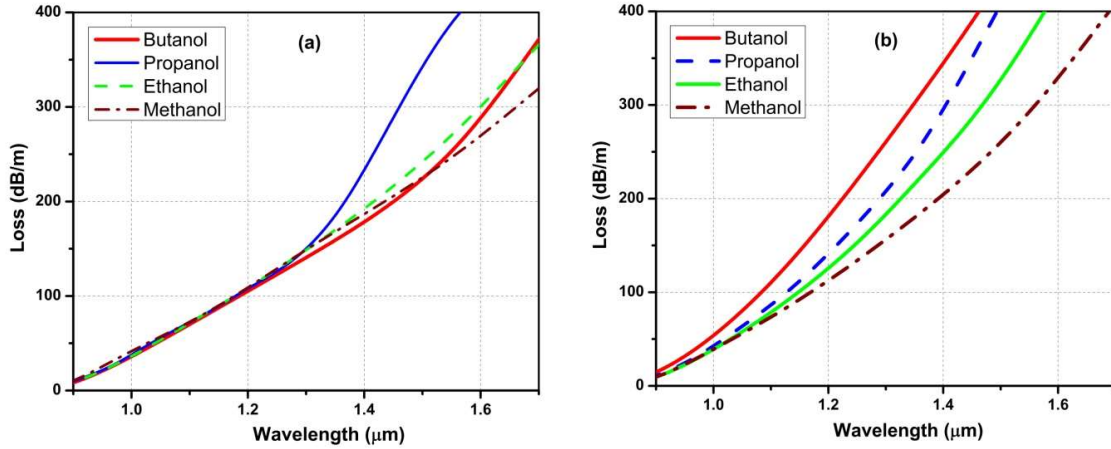


Fig. 6. The dependence of the confinement loss on the wavelength of the fiber with various air hole diameters infiltrated with alcoholic liquids. a) $d = 1.42 \mu\text{m}$ and $\Lambda = 3.26 \mu\text{m}$ and b) $d = 1 \mu\text{m}$ and $\Lambda = 5 \mu\text{m}$.

Table 6. The value of the confinement loss of the fiber with various air hole diameters at $1.55 \mu\text{m}$ wavelength infiltrated with alcoholic liquids.

| λ (μm) | Liquids | L_c (dB/m) | |
|-----------------------------|----------|---|---|
| | | $d = 1.42 \mu\text{m}$ and $\Lambda = 3.26 \mu\text{m}$ | $d = 1 \mu\text{m}$ and $\Lambda = 5 \mu\text{m}$ |
| 1.55 | Butanol | 230.858223 | 447.199955 |
| | Propanol | 354.901137 | 421.062537 |
| | Ethanol | 248.769953 | 338.318116 |
| | Methanol | 230.322546 | 268.088848 |

Table 6 indicates the confinement loss of the PCF with various air hole diameters at $1.55 \mu\text{m}$ wavelength infiltrated with alcoholic liquids. The confinement loss value increases when the diameter of air holes decreases due to the decrease of absorption ability. With the diameter of air holes of $1.42 \mu\text{m}$, the highest and lowest confinement loss of propanol and methanol is 354.901137 dB/m and 230.322546 dB/m , respectively. When the diameter of air holes is $1.0 \mu\text{m}$, the value of

the confinement loss is reduced from butanol, propanol, ethanol to methanol, the highest value is 447.199955 dB/m for butanol and the lowest value is 268.088848 dB/m for methanol. The smallest confinement loss and the flattest dispersed curve is convenient in application for supercontinuum generation.

IV. CONCLUSION

The properties of these PCF such as the effective refractive index, effective mode area, dispersion and confinement loss of the fibers were studied numerically and analyzed with different alcoholic liquids. The influence on the diameters and lattice constants of air holes is investigated, too. Compared with the fibers infiltrated with different alcoholic liquids, the PCF infiltrated with ethanol and butanol showed better near zero flattened dispersion property at 1.42 μm and 1 μm wavelength respectively. With diameters and lattice constants of air holes equal to 1.42 μm and 3.26 μm , the smallest dispersion of PCF filled with ethanol of 5.91075308 (ps.(nm.km)⁻¹) and methanol of 19.3592474 (ps.(nm.km)⁻¹). The highest ZDW of the PCF infiltrated with ethanol and methanol is 1.24604224 μm and 1.22405714 μm , respectively. Specially, the value of effective refractive index, effective mode area, dispersion and confinement loss decrease in an orderly manner from butanol, propanol, ethanol to methanol. Hence, the characteristics of a PCF fiber infiltrated with different alcoholic liquids and so the geometry of its microstructure, is one of the key factors for supercontinuum generation.

REFERENCES

- [1] P. Yeh, A. Yariv, E. Marom, *J. Opt. Soc. Am.* **68** (1978) 1196.
- [2] J. C. Knight, T. A. Birks, P. St. J. Russell, and D. M. Atkin, *Opt. Lett.* **21** (1996) 1547.
- [3] K. Ahmed, M. Morshed, S. Asaduzzaman, M.F.H. Arif, *Optik* **131** (2017) 687.
- [4] K. Saitoh and M. Koshiba, *J. Lightwave Technol.* **23** (2005) 3580.
- [5] N. A. Mortensen, J. R. Jensen, P. M. W. Skovgaard, and J. Broeng, *IEEE Photon. Technol. Lett.* **14** (2002) 1094.
- [6] T. A. Birks, J. C. Knight, and P. S. J. Russell, *Opt. Lett.* **22** (1997) 961.
- [7] L. B. Shaw, V.Q. Nguyen, J.S. Sanghera, I.D. Aggarwal, P.A. Thielen, and F.H. Kung, *Advanced Solid-State Photonics* **98** (2005) 864.
- [8] Tigran Baghdasaryan, Thomas Geernaert, Francis Berghmans, and Hugo Thienpont, *Opt. Express* **19** (2011) 7705.
- [9] Y. E. Monfared, A. M. Javan and A. M. Kashani, *Optik* **124** (2013) 7049.
- [10] Klimczak, M., Stepniowski, G., Bookey, H., Szolno, A., Stepien, R., Pysz, D., Kar, A., Waddie, A., Taghizadeh, M.R., Buczynski, R., *Optics Lett.* **38** (2013) 4679.
- [11] Jacek Pniewski, Tomasz Stefaniuk, Hieu Le Van, Van Cao Long, Lanh Chu Van, RafałKasztelanic, Grzegorz Stêpniewski, Aleksandr Ramaniuk, Marek Trippenbach, and Ryszard Buczyński, *Applied Optics* **55** (2016) 5033.
- [12] L. Chu Van, T. Stefaniuk, R. Kasztelanic, V. Cao Long, M. Klimczak, H. Le Van, M. Trippenbach, R. Buczynski, *Proc. of SPIE* **9816** (2015) 981600-1.
- [13] Khoa Dinh Xuan, Lanh Chu Van, Van Cao Long, Quang Ho Dinh, Luu Van Mai, Marek Trippenbach, Ryszard Buczyński, *Opt. Quant. Electron.* **49** (2017) 87.
- [14] Chu Van Lanh, Van Thuy Hoang, Van Cao Long, Krzysztof Borzycki, Khoa Dinh Xuan, Vu Tran Quoc, Marek Trippenbach, Ryszard Buczyński and Jacek Pniewski, *Laser Phys.* **29** (2019) 075107.
- [15] T. Larsen, A. Bjarklev, D. Hermann, and J. Broeng, *Opt. Express* **11** (2003) 2589.
- [16] C. Yu and J. Liou, *Opt. Express* **17** (2009) 8729.
- [17] F. Du, Y.-Q. Lu, and S.-T. Wu, *Appl. Phys. Lett.* **85** (2004) 2181.
- [18] D. Noordegraaf, L. Scolari, J. Lægsgaard, L. Rindorf, and T. T. Alkeskjold, *Opt. Express* **15** (2007) 7901.
- [19] K. M. Gundu, M. Kolesik, J. V. Moloney, K. S. Lee, *Opt. Express* **14** (2006) 6870.
- [20] P. D. Rasmussen, J. Lægsgaard, and O. Bang, *J. Opt. Soc. Am. B* **23** (2006) 2241.

- [21] J. Park, D. Kang, B. Paulson, T. Nazari, and K. Oh, *Opt. Express* **22** (2014) 17320.
- [22] C. Yu, J. Liou, S. Huang, and H. Chang, *Opt. Express* **16** (2008) 4443.
- [23] R. Zhang, J. Teipel, and H. Giessen, *Opt. Express* **14** (2006) 6800.
- [24] Z. Zhu and T. Brown, *Opt. Express* **8** (2001) 547.
- [25] P. P. Ho and R. R. Alfano, *Phys. Rev. A* **20** (1979) 2170.
- [26] Hieu Van Le, Van Long Cao, Hue Thi Nguyen, An Manh Nguyen, Ryszard Buczyński and Rafał Kasztelaniec, *Laser Phys.* **28** (2018) 115106.
- [27] Lumerical Eigenmode Expansion (EME) Solver, <https://www.lumerical.com/tcad/products/mode/EME>, accessed 29 August 2016.
- [28] K. Moutzouris, M. Papamichael, S. Betsis, I. Stavarakas, G. Hloupis, D. Triantis, *Appl. Phys. B* **116** (2014) 617.
- [29] I. H. Malitson, *J. Opt. Soc. Am.* **55** (1965) 1205.
- [30] G. Agrawal, *Nonlinear Fiber Optics*, 3rd ed.; Academic Press: New York, (2001).
- [31] N. Naddi, E. Mahammed, and K. L. N. Ksihore, *IOSR J. Electron. Commun. Eng.* **12** (2017) 9.
- [32] T. P. White, R. C. McPhedran, C. M. de Sterke, L. C. Botten, and M. J. Steel, *Opt. Lett.* **26** (2001) 1660.
- [33] S. Fatema, R. Absar, M. Istiaque Reja, and J. Akhtar, *J. Opt. Commun.* **410** (2018) 396.
- [34] Jingli Lei, Shanglin Hou, Yanjun Liu, and Xiaoxiao Li, *Progress In Electromagnetics Research Symposium Proceedings*, Guangzhou, China, Aug. 25-28 (2014).
- [35] R. E. Kristiansen, K. P. Hansen, J. Broeng, P. M. W. Skovgaard, M. D. Nielsen, A. Petersson, T. P. Hansen, B. Mangan, C. Jakobsen, and H. R. Simonsen, *Proc. Reunion Espanola de Optoelectronica (Elche)* **38** (2005) 37.
- [36] M. D. Nielsen, J. R. Folkenberg, and N. A. Mortensen, *Electron. Lett.* **39** (2003) 25.
- [37] J. M. Dudley, G. Genty, and S. Coen, *Rev. Mod. Phys.* **78** (2006) 1135.
- [38] M. L. V. Tse, P. Horak, F. Poletti, N. G. R. Broderick, J. H. V. Price, J. R. Hayes, D. J. Richardson, *Opt. Express* **14** (2006) 4445.